



RAPID COMMUNICATION

Mechano-sensitive TET1s inhibits endothelial athero-susceptible phenotype through regulating YAP phosphorylation

Atherosclerosis is a chronic progressive disease and one of the major causes of cardio-cerebral vascular diseases. Accumulating evidence indicates that endothelial dysfunction is the initiating step in atherosclerosis. The pattern of local blood flow becomes disturbed (low and oscillatory shear stress [OSS]) in the curved or branched segments of the arterial tree, causing endothelial cells (ECs) to exhibit athero-susceptible phenotypes, such as hyperproliferation and inflammation. By contrast, laminar blood flow in the straight parts of the arterial tree (high and unidirectional laminar shear stress [LSS]) causes ECs to act in a way that protects against atherosclerosis. The short isoform of Tet methylcytosine dioxygenase 1 (TET1s)^{1,2} is implicated in early embryonic development, cancer, and the mammalian nervous system.^{1–3} However, whether TET1s expression in ECs can regulate the initiation and development of atherosclerosis has not been explored. In the present study, we provided *in vivo* and *in vitro* evidence that atherogenic OSS reduced TET1s expression in ECs. The reduction in TET1s expression in turn induced the inflammatory and proliferative responses of ECs and ultimately led to atherosclerotic lesion formation. In addition, we demonstrated that TET1s prevented the OSS-mediated nuclear translocation of yes-associated protein (YAP) by increasing its phosphorylation at serine 127. These findings support the protective role of TET1s in modulating endothelial athero-susceptible phenotypes and atherogenesis.

In vivo animal models and an *in vitro* parallel-plate flow chamber system were used to evaluate the effect of disturbed flow on TET1s expression. Especially, a partial carotid ligation mouse model was used to show that TET1s mRNA and protein expression were lower in the left carotid artery (LCA, which had disturbed blood flow) than in the contralateral right carotid artery (RCA, which retained

unidirectional blood flow) 48 h post-ligation (Fig. 1A, B; Fig. S1A, S1B). In addition, we demonstrated that TET1s mRNA and protein levels were reduced in the *in-vitro*-cultured human umbilical vein endothelial cells (HUVECs) placed under OSS (Fig. 1C; Fig. S1C, D). To further investigate the role of TET1s in atherogenesis, we obtained TET1 and TET1s double-knockout mice (*Tet1*^{-/-}), and TET1 knockout mice (*Tet1*^{cs/cs}) on an *ApoE*^{-/-} background. These mice were fed a high-fat diet (HFD) for 8 weeks to generate the atherosclerosis model. The *ApoE*^{-/-} mice on an HFD were used as the controls. Aortic-root staining showed that *Tet1*^{-/-} *ApoE*^{-/-} mice had more lipid accumulation than the other two groups (Fig. 1D, E), which indicated that TET1s might influence hemodynamic force-related atherosclerosis.

A series of functional assays were then performed to determine the role of TET1s in ECs. Knockdown of TET1s with siRNA (Fig. S2A) markedly increased EC numbers (Fig. 1F) and the proliferating cell nuclear antigen (PCNA) protein levels (Fig. S2B). By contrast, adenovirus-induced TET1s overexpression (Fig. S2C) reduced PCNA levels in ECs (Fig. S2D). Application of OSS to HUVECs *in vitro* promoted cell proliferation to a greater extent than when LSS was applied (Fig. 1G). However, TET1s overexpression alleviated the OSS-mediated abnormal proliferation of HUVECs (Fig. 1G). We also found that the knockdown of TET1s up-regulated the expression of intercellular adhesion molecule 1 (ICAM-1) and vascular cell adhesion molecule 1 (VCAM-1) (Fig. 1H; Fig. S2E–G). High ICAM-1 and VCAM-1 expression in turn contributed to increased leukocyte adhesion and endothelial inflammation (Fig. S2H). Moreover, the inflammatory state established following lipopolysaccharide (LPS) treatment was attenuated on TET1s overexpression. This was evidenced by lowered ICAM-1 and VCAM-1 expression (Fig. 1I; Fig. S2I–K) and reduced THP-1 monocyte adhesion

Peer review under responsibility of Chongqing Medical University.

<https://doi.org/10.1016/j.gendis.2023.01.029>

2352-3042/© 2023 The Authors. Publishing services by Elsevier B.V. on behalf of KeAi Communications Co., Ltd. This is an open access article under the CC BY-NC-ND license (<http://creativecommons.org/licenses/by-nc-nd/4.0/>).

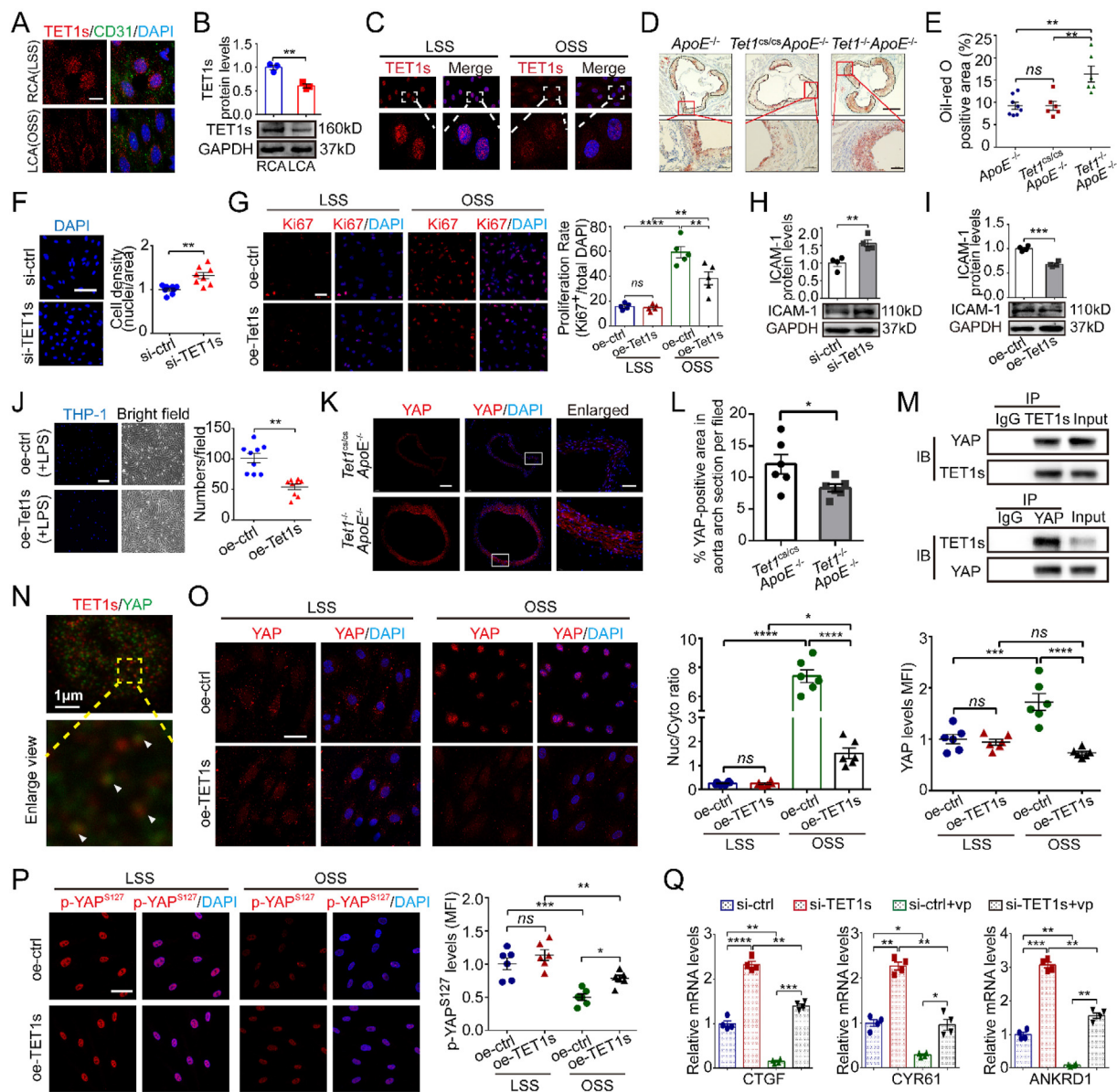


Figure 1 Mechanosensitive TET1s prevents endothelial dysfunction in response to oscillatory shear stress (OSS) by dampening YAP activity. (A) En face staining for TET1s in the carotid arteries of wildtype (WT) mice 48 h post-ligation; bar = 10 μ m. Mean fluorescent intensity (MFI) of TET1s staining was quantified for statistical analysis; data are shown as the mean \pm SEM, $**P < 0.01$ (Student's *t*-test), $n = 5$. (B) Western blot analysis of TET1s expression in the right carotid artery (RCA) and left carotid artery (LCA) after partial carotid ligation; data are shown as the mean \pm SEM, $**P < 0.01$ (Student's *t*-test), $n = 3$. (C) Immunofluorescence staining of TET1s in HUVECs exposed to laminar shear stress (LSS) or OSS; bar = 20 μ m. (D) Representative images of Oil-red O staining of aortic root sections. Dashed line indicates the plaque area; bar = 500 μ m. Enlarged view; bar = 100 μ m. (E) Quantification of the Oil-red-O-positive area; data are shown as the mean \pm SEM, $**P < 0.01$ (one-way ANOVA with Tukey's post hoc test). ns, not significant, $n \geq 6$. (F) Cell density was quantified by counting nuclei 48 h post-transfection; bar = 100 μ m. Data are shown as the mean \pm SEM, $**P < 0.01$ (Student's *t*-test), $n = 8$. (G) Immunofluorescence staining of Ki67 in HUVECs exposed to LSS or OSS for 6 h; bar = 50 μ m. The proliferation rate of cells in the left panel was analyzed; data are shown as the mean \pm SEM, $**P < 0.01$, $****P < 0.0001$ (one-way ANOVA with Tukey's post hoc test). ns, not significant, $n = 5$. (H) Western blot analysis of ICAM-1 expression HUVECs after TET1s knockdown; data are shown as the mean \pm SEM, $**P < 0.01$ (Student's *t*-test), $n = 4$. (I) Western blot analysis of ICAM-1 expression in TET1s-overexpressing HUVECs; data are shown as the mean \pm SEM, $***P < 0.001$ (Student's *t*-test), $n = 4$. (J) Representative images of adhesive THP-1 cells (labeled with Hoechst 33342); bar = 200 μ m. Quantification of

(Fig. 1J). Collectively, these results suggest that TET1s exerted anti-proliferative and anti-inflammatory functions in ECs upon OSS exposure.

Recent studies have linked YAP to the pathological process of atherosclerosis.⁴ Therefore, to further understand the underlying mechanisms of the TET1s-regulated function of EC, we investigated the relationship between TET1s and YAP. We found that YAP was more highly expressed in the aortic arch (AA) of *Tet1*^{-/-} *ApoE*^{-/-} mice than in that of *Tet1*^{cs/cs} *ApoE*^{-/-} mice (Fig. 1K, L) and that TET1s knockdown increased YAP expression in ECs (Fig. S3A, C). Moreover, a physical interaction between TET1s and YAP was confirmed by co-immunoprecipitation and immunofluorescence co-localization (Fig. 1M, N).

The cellular localization of YAP is regulated by shear stress. Hence, we assessed how TET1s regulated YAP under shear stress conditions and found that the nuclear translocation of YAP was markedly increased in ECs following TET1s knockdown (Fig. S3A, B). Moreover, immunofluorescence staining showed that OSS significantly increased the nuclear accumulation and expression of YAP, whereas LSS had the opposite effect (Fig. 1O). Intriguingly, TET1s overexpression inhibited the OSS-mediated nuclear translocation and expression of YAP (Fig. 1O).

The activation and cellular localization of YAP under different conditions of shear stress are dependent on its phosphorylation at specific amino-acid residues.⁵ We found that the knockdown of TET1s significantly decreased YAP phosphorylation at serine 127 (Fig. S4A). We next determined the phosphorylation of YAP serine 127 (p-YAP^{S127}) under shear stress and found that OSS induction reduced p-YAP^{S127} levels, which were restored by TET1s overexpression (Fig. 1P). Thus, our results indicate that TET1s modulated the nuclear localization and expression of YAP by regulating YAP phosphorylation in response to shear stress.

We then proceed to confirm the effect of TET1s on YAP activation. The results showed that the expression of the *CTGF*, *CYR61*, and *ANKRD1* (YAP downstream target genes) was increased in HUVECs after TET1s knockdown (Fig. 1Q) but reduced in TET1s-overexpressing HUVECs (Fig. S4B).

Finally, we evaluated whether the inhibition of YAP activity with verteporfin (vp) was sufficient to prevent the EC dysfunction caused by TET1s deficiency. As expected, vp treatment markedly suppressed the expression of *CTGF*, *CYR61*, and *ANKRD1* and reduced their up-regulation in response to TET1s knockdown (Fig. 1Q). Meanwhile, vp also attenuated the expression of *PCNA*, *ICAM-1*, and *VCAM-1* in ECs, following TET1s knockdown (Fig. S4C). Taken together, these results indicate that TET1s mediated EC proliferation and the inflammatory response to shear stress, at least in part, by modulating YAP activity.

In the present study, we reported that TET1s was sensitive to hemodynamic forces and modulated athero-related endothelial phenotypes in ECs under disturbed flow. Mechanistically, we showed that TET1s bound to and inhibited YAP activity by increasing p-YAP^{S127} levels. This subsequently repressed the expression of EC proliferation- and inflammation-related genes, which are typically up-regulated in response to mechanical shear stress. Collectively, our findings reveal a novel role for TET1s in the regulation of athero-susceptible EC phenotypes, which may contribute to the development of preventative and therapeutic strategies for atherosclerosis. Further mechanistic insights into how TET1s modulates YAP activity under different hemodynamic conditions are needed.

Author contributions

GX Wang, JH Qiu, and L Huang conceived the idea and designed the experiments. L Huang performed experiments and analyzed and interpreted the data. L Huang, JH Qiu, and DX Lei wrote and revised the paper. K Qu, C Wang, WH Yan, TH Li, and ZJ Hou participated in part of the experiments.

Conflict of interests

The authors have no relevant financial or non-financial interests to disclose.

adhesive THP-1 cell number per unit visual field; data are shown as the mean \pm SEM, $**P < 0.01$ (Student's *t*-test), $n = 9$. (K) Immunofluorescence staining of YAP in the aorta arch section of *Tet1*^{-/-} *ApoE*^{-/-} mice or *Tet1*^{cs/cs} *ApoE*^{-/-} mice on a high-fat diet for 2 weeks; bar = 200 μ m. Enlarged view, bar = 50 μ m. (L) Quantitative analysis of YAP levels in the aorta section; data are shown as the mean \pm SEM, $*P < 0.05$ (Student's *t*-test), $n = 6$. (M) Direct interaction between TET1s and YAP, detected by co-immunoprecipitation. (N) Immunofluorescence co-localization of TET1s and YAP. (O) Immunofluorescence staining of YAP in infected HUVECs exposed to LSS or OSS for 6 h, bar = 40 μ m. Right panel 1: Quantitative analysis of the nuclear-cytoplasmic ratio of YAP. Panel 2: Quantification of YAP MFI; data are shown as the mean \pm SEM, $*P < 0.05$, $***P < 0.001$, $****P < 0.0001$ (one-way ANOVA with Tukey's post hoc test). ns, not significant, $n = 6$. (P) Immunofluorescence staining of p-YAP^{S127} in transfected HUVECs exposed to LSS or OSS for 6 h, bar = 40 μ m. Right panel: Quantification of p-YAP^{S127} MFI; data are shown as the mean \pm SEM, $*P < 0.01$, $**P < 0.01$, $***P < 0.001$ (one-way ANOVA with Tukey's post hoc test). ns, not significant, $n = 6$. (Q) HUVECs were transfected with the indicated siRNA for 48 h, with or without verteporfin (vp, a YAP inhibitor) treatment (10 μ M, 24 h). Quantitative real-time (qRT)-PCR analysis of YAP target gene (*CTGF*, *CYR61*, and *ANKRD1*) expression normalized to *GAPDH*; data are shown as the mean \pm SEM, $*P < 0.05$, $**P < 0.01$, $***P < 0.001$, $****P < 0.0001$ (one-way ANOVA with Tukey's post hoc test), $n = 4$.

Funding

The work is supported by the Natural Science Foundation of China (No. 31971242, 12032007), Chongqing Science and Technology Bureau (China) (No. cstc2019jcyj-zdxmX0028, cstc2020jscx-msxmX0132), Chongqing Postdoctoral Science Foundation (China) (No. cstc2021jcyj-bsh0208, cstc2021jcyj-bshX0181), and Fundamental Research Funds for Central Universities (China) (No. 2021CDJCGJ007).

Acknowledgements

We are grateful to Dr. Wei Xie at Tsinghua university for sharing *Tet1^{cs/cs}* mice and Dr. Chen Dong at Tsinghua University for sharing *Tet1^{-/-}* mice. We also appreciate the other staff of the Public Experiment Center of State Bio-industrial Base (Chongqing) for providing technical support and assistance in data collection and analysis.

Appendix A. Supplementary data

Supplementary data to this article can be found online at <https://doi.org/10.1016/j.j.gendis.2023.01.029>.

References

- Zhang W, Xia W, Wang Q, et al. Isoform switch of TET1 regulates DNA demethylation and mouse development. *Mol Cell*. 2016; 64(6):1062–1073.
- Good CR, Madzo J, Patel B, et al. A novel isoform of TET1 that lacks a CXXC domain is overexpressed in cancer. *Nucleic Acids Res*. 2017;45(14):8269–8281.
- Greer CB, Wright J, Weiss JD, et al. *Tet1* isoforms differentially regulate gene expression, synaptic transmission, and memory in the mammalian brain. *J Neurosci*. 2021;41(4):578–593.
- Wang KC, Yeh YT, Nguyen P, et al. Flow-dependent YAP/TAZ activities regulate endothelial phenotypes and atherosclerosis. *Proc Natl Acad Sci U S A*. 2016;113(41):11525–11530.
- Wang L, Luo JY, Li B, et al. Integrin-YAP/TAZ-JNK cascade mediates atheroprotective effect of unidirectional shear flow. *Nature*. 2016;540(7634):579–582.

Lu Huang ^{a,b}, Kai Qu ^a, Caihong Wang ^a, Daoxi Lei ^{a,c},
Wenhua Yan ^{a,d}, Tianhan Li ^a, Zhengjun Hou ^{a,b},
Juhui Qiu ^{a,**}, Guixue Wang ^{a,*}

^a Key Laboratory for Bioreheological Science and Technology of Ministry of Education, State and Local Joint Engineering Laboratory for Vascular Implants, Bioengineering College of Chongqing University, Chongqing 400030, China

^b School of Advanced Manufacturing Engineering, Chongqing University of Posts and Telecommunications, Chongqing 400065, China

^c Department of Ophthalmology, Chongqing Hospital of Traditional Chinese Medicine, Chongqing 400021, China

^d The Second Affiliated Hospital of Chongqing Medical University, Chongqing 400010, China

*Corresponding author.

**Corresponding author.

E-mail addresses: jhqu@cqu.edu.cn (J. Qiu), guixue_wang@126.com (G. Wang)

2 September 2022
Available online 4 April 2023